JOURNAL OF THEORETICAL
AND APPLIED MECHANICS
https://doi.org/10.15632/jtam-pl/208484
ONLINE FIRST

IMPACT OF HONEYCOMB STRAIGHTENER PARAMETERS ON OPERATION IN A STRAIGHT DUCT

Emil SMYK[1*], Michał STOPEL[1], Adam RACHWALSKI[2]

[1] *Bydgoszcz University of Science and Technology, Bydgoszcz, Poland*
[2] *Hanplast Sp. z o.o., Bydgoszcz, Poland*

*corresponding author, *emil.smyk@pbs.edu.pl*

The influence of the honeycomb diameter and straightener length on performance was investigated. Velocity profiles were measured using a hot-wire anemometer, and pressure losses were also recorded. The straighteners were placed 10D downstream of the fan. Measurements were conducted at Reynolds numbers of 10000, 15000, 30000, 45000. Additionally, two methods were proposed to assess the influence of straighteners on the shape of the velocity profile. The results showed that at Reynolds numbers of 10000 and 15000, straighteners had only a minor effect on reducing turbulence intensity and relaminarizing the velocity profile. In contrast, at higher Reynolds numbers, their impact was significant.

Keywords: pressure drop; Fanning friction factor; head pressure losses; channels; inner flow.

1. Introduction

Stream straighteners are simple devices used in ventilation ducts, HVAC systems, jet engines, industrial pipelines, scientific research, tanks, and overflow vessels. They are designed to correct unexpected and unwanted flow profile effects, often caused by the absence of required straight sections upstream and downstream of the measurement point. Also known as stream conditioners, these devices reduce hydraulic entrance length and decrease turbulence intensity, enabling the required velocity profile. Some types of stream straighteners have been described in (International Organization for Standardization, 2022). However, due to their simple manufacturing process, the most common flow straighteners are those in the shape of a honeycomb (Hrúz *et al.*, 2020).

The earliest paper on flow straighteners found is the one by Bradshaw (1965). He cited earlier work (from 1959), but access to it could not be obtained. He investigated wind tunnel screens. Lumley and McMahon (1967) demonstrated that this straightener significantly reduced turbulence intensity. Tan-Atichat *et al.* (1982) proposed using screens and grids to decrease turbulence, showing that an appropriately selected screen and a grid (acting as a turbulence generator) could shorten turbulence decay distance by a factor of four. Groth and Johansson (1988) examined a cascade of the screens in a wind tunnel and concluded that using a major loss factor as an efficiency determinant was incorrect since different screen arrangements with

Ministry of Science and Higher Education
Republic of Poland

This publication has been funded by the Polish Ministry of Science and Higher Education under the Excellent Science II programme "Support for scientific conferences".
The content of this article was presented during the 61st Symposium "Modelowanie w mechanice" (Modelling in Mechanics), Szczyrk, Poland, March 2–5, 2025.

varying major loss factors could yield the same turbulence reduction. Laws (1990) introduced a new type of straightener/conditioner featuring holes of different diameters in the outer and inner rings. He suggested that the minimum straightener length should be D/8, where D is the channel diameter, and noted that straightener length does not significantly affect performance.

Xiong *et al.* (2003) compared two perforated plates and a tube bundle, showing that perforated plates act as turbulence grids, producing homogeneous and quasi-isotropic turbulence more efficiently than tube bundles. The turbulence field does not reach equilibrium even at a downstream position of 50 diameters. Saunders *et al.* (2004) tested honeycomb straighteners with screens in a wind tunnel and, like Xiong *et al.* (2003), found that turbulence initially increased downstream of the flow conditioners before decreasing. Hamzah *et al.* (2021) numerically investigated a honeycomb straightener in a wind tunnel and found that straighteners improved flow parameters, increasing the usable test. However, they simulated the straightener as a porous medium, making their results applicable only to simulation.

Kühnen *et al.* (2018) demonstrated that flow relaminarization can be achieved by reducing wall shear using two specially designed passive conditioners. El Drainy *et al.* (2009) studied tangential vortex induction behind the Zenker plates, showing that tangential velocity depends on plate thickness and disappears with increased straightener length. Sun *et al.* (2023; 2025) investigated the role of the honeycomb in the relaminarization of the synthetic jet. They show that the honeycomb straightener can reduce the periodic and random velocity fluctuation even in periodic phenomena such as synthetic jets. They also pointed out the need to properly select the length and diameter of the straightener. Jurga *et al.* (2024) investigated honeycomb straighteners both upstream and downstream of an elbow. Their studies demonstrated that the straightener suppresses the secondary flow generated by the elbow and positively influences the velocity profile. Flow through an elbow is one of the fundamental types of configuration analyzed in the literature, for example, in (Dutta *et al.*, 2025; Smyk *et al.*, 2024).

Kühnen *et al.* (2018) suggest that the objective of flow relaminarization is to minimize energy consumption, given that laminar flow results in reduced losses compared to turbulent flow. Apart from reduced flow losses, a symptom of laminar flow is the shape of the velocity profile, expressed by Prandtl's power law formula (Salama, 2021). Kühnen *et al.* (2018) also suggest that a paraboloidal velocity profile indicates relaminarization of the flow. Flow relaminarization is achieved by locally increasing shear stresses (Jurga *et al.*, 2024; Kühnen *et al.*, 2018), and can be classified as a passive flow control method. Flow straighteners are similar in design to filters and consist of small channels (Kaminski *et al.*, 2025). These can also be used as stream straighteners. Passive flow control methods involving the local increase of shear stresses are also employed in external flows (Dróżdż *et al.*, 2025; Klotz *et al.*, 2024), where the objective is to attain an optimal velocity profile shape.

In the analyzed papers, the straighteners were investigated mainly in wind tunnels and the turbulence and profile disturbance were generated very often by the grid. Flow straighteners are mainly used in pipelines, and based on the literature, it is difficult to indicate an unambiguous way of designing and the scope of application of straighteners. For example, to determine what Reynolds numbers of flow they should be used for. The purpose of this article is to discuss the influence of the channel diameter and length of honeycomb straighteners on their performance. The study also used a different vortex generator than in the remaining literature, as it was an axial fan, which is more consistent with the structure and characteristics of real-life cases of using straighteners in industry. The data were presented in a manner that makes it possible to create a numerical model and extend the research to additional cases.

2. Materials and methods

The impact of the honeycomb straighteners on flow parameters was assessed using a test channel equipped with measurement devices, as shown in Fig. 1. Honeycombs were manufac-

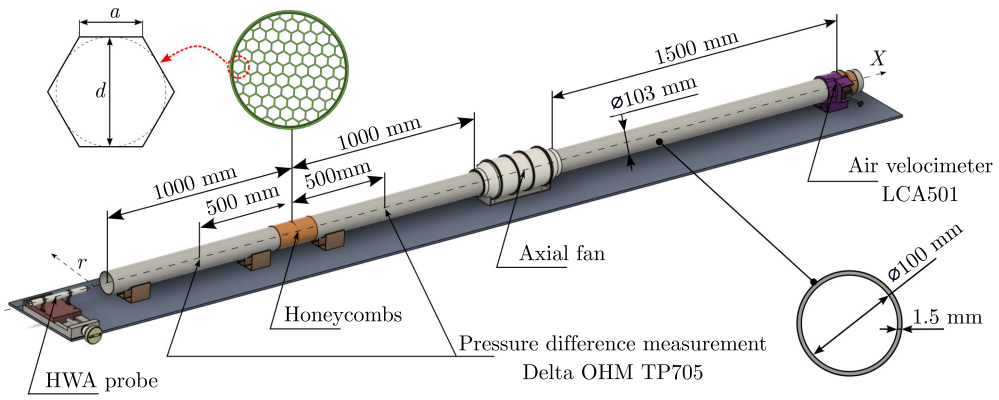

Fig. 1. Test channel schematic with the measurement equipment.

tured with 3D print technology with polylactide acid (PLA) and placed in the straight channel 1000 mm behind the axial fan (Soler&Palau TD-250) controlled by a Soler&Palau REB-1 speed controller. The fan acted as a turbulence generator. To evaluate the effect of straighteners on the flow parameters, the velocity profile in the channel was measured using a MiniCTA 55T30 hot-wire anemometer (HWA) with a 55P16 single-wire probe and a NI9215 data acquisition device. Velocity profiles were measured 1000 mm downstream of the honeycomb. The anemometer was calibrated for velocity measurements ranging from 1.5 m/s to 26 m/s. Temperature correction was applied, and the velocity measurement accuracy was within ±6 % of the reading. The HWA probe was placed 1 mm behind the channel outlet, and positioning was performed using a micrometer screw. The inner diameter of the pipe (channel diameter) was $D = 100$ mm, and the outer diameter of the pipe was $D_{\text{out}} = 103$ mm. The pressure drop on the honeycomb was measured with the differential pressure probe Delta OHM TP705-10MBD (the measurement range was 1000 Pa, the accuracy was ±0.5 % of full scale, and the measurement resolution was 1 Pa) connected to Delta OHM DH 2124.2 pressure meter. The pressure drop was measured at a distance of 1000 mm, as shown in Fig. 1. Mean velocity was determined using an Airflow LCA501 air velocity meter (measurement range: 0.25 m/s–30 m/s, accuracy: ±1 % of reading) placed 1500 mm upstream of the fan.

Measurements were conducted for six honeycomb straighteners and a control channel without straighteners. The parameters of the honeycomb straighteners are presented in Table 1. They covered four different Reynolds numbers Re = 10000, 15000, 30000, 45000, calculated as

$$\text{Re} = \frac{UD}{\nu}, \tag{2.1}$$

where U is a mean velocity [m/s], and ν is a kinematic viscosity equal of $\nu = 15.16 \cdot 10^{-6}$ m^2/s for the air temperature of 21 °C and the air humidity of 37 %.

Table 1. Dimensions of the honeycomb straighteners.

Case	Honeycomb diameter d [mm]	Honeycomb side length a [mm]	Straightener length L [mm]
Without	–	–	–
D10L5	10	5.77	5
D10L10	10	5.77	10
D10L20	10	5.77	20
D10L40	10	5.77	40
D5L20	5	2.89	20
D20L20	20	11.55	20

Velocity profiles were measured directly at the fan outlet and at a distance of 1000 mm behind the fan (where the straighteners were installed to illustrate canes in flow parameters within a straight channel).

The velocity measurement with the HWA was conducted at a sampling frequency of $f = 50\,\text{kHz}$ for 1 s at each measurement point. This setup allowed both velocity and turbulence intensity measurements. The mean velocity (U), standard deviation of the velocity (U_{rms}) and the turbulence intensity (Tu) of the flow were determined as

$$U = \frac{1}{N}\sum_{i=1}^{N} u_i, \qquad U_{\text{rms}} = \sqrt{\frac{1}{N-1}\sum_{i=1}^{N}(u_i - U)^2}, \qquad Tu = \frac{U_{\text{rms}}}{U}, \tag{2.2}$$

where u_i is a measured velocity series sample [m/s], N is the number of series samples ($N = 50000$).

This study investigated the impact of honeycomb straighteners on the velocity profile. To analyze this effect, Prandtl's power law formula was applied, which describes the velocity profile in turbulent flow (Salama, 2021):

$$\frac{U}{U_{\max}} = \left(1 - \frac{r}{R}\right)^{1/n}, \tag{2.3}$$

where $U_{\max}$ is the maximum velocity value [m/s], r is the radial distance from the axis (see Fig. 1) [m], R is a channel radius ($R = D/2 = 50\,\text{mm}$), n is an exponent depending on the Reynolds number. The exponent n was calculated for each measured velocity profile in such a way as to satisfy the relationship:

$$\left(\frac{1}{U_{\max}^2}\sum\left(U(r)_{\text{experimental}} - U(r)_{\text{theoretical}}\right)^2\right) \to 0, \tag{2.4}$$

where $U_{\text{theoretical}}$ was calculated from Eq. (2.3). The Solver add-in in Microsoft Excel was used to find the value of exponent n.

3. Results

3.1. Profiles in a straight channel

Figure 2 presents the velocity profile measured directly on the outlet of the fan (Fig. 2a), 1000 mm downstream of the fan (Fig. 2b), and 2000 mm downstream of the fan (Fig. 2c). The change in the velocity profile shape and the turbulence intensity with increasing distance from the fan was evident for all Reynolds numbers. The velocity profile becomes more rectangular as the distance from the fan increases. Additionally, for Re = 10000 a distinct rounding of the profile near the duct wall is observed. Generally, higher Reynolds numbers correspond to flatter velocity profiles (Salama, 2021). However, as shown in Fig. 2c, the velocity profiles for Re = 10000 and 15000 appear flatter than those for Re = 30000 and 45000. This discrepancy is attributed to greater irregularities in the velocity profile at high Reynolds numbers compared to lower ones. It is expected that using a longer channel would result in further profile flattering at high Reynolds numbers.

As expected, higher Reynolds numbers correspond to increased turbulence levels. The highest turbulence intensity was observed near the walls and was due to shear effects (Hwang, 2024). The turbulence intensity near the wall, relative to the duct axis, is evident for Re = 10000, 15000, and 30000. However, for all cases, turbulence intensity decreased with increasing distance from the fan. The change in turbulence intensity at the duct axis between the fan outlet and 2000 mm downstream is as follows: from 2.78 % to 0.86 % for Re = 10000; from 3.68 % to 0.52 % for Re = 15000; from 17.84 % to 5.85 % for Re = 30000; from 13.52 % to 5.93 % for Re = 45000.

The direct correlation between turbulence intensity and the Reynolds number confirms the feasibility of using a duct fan as a vortex generator in the flow.

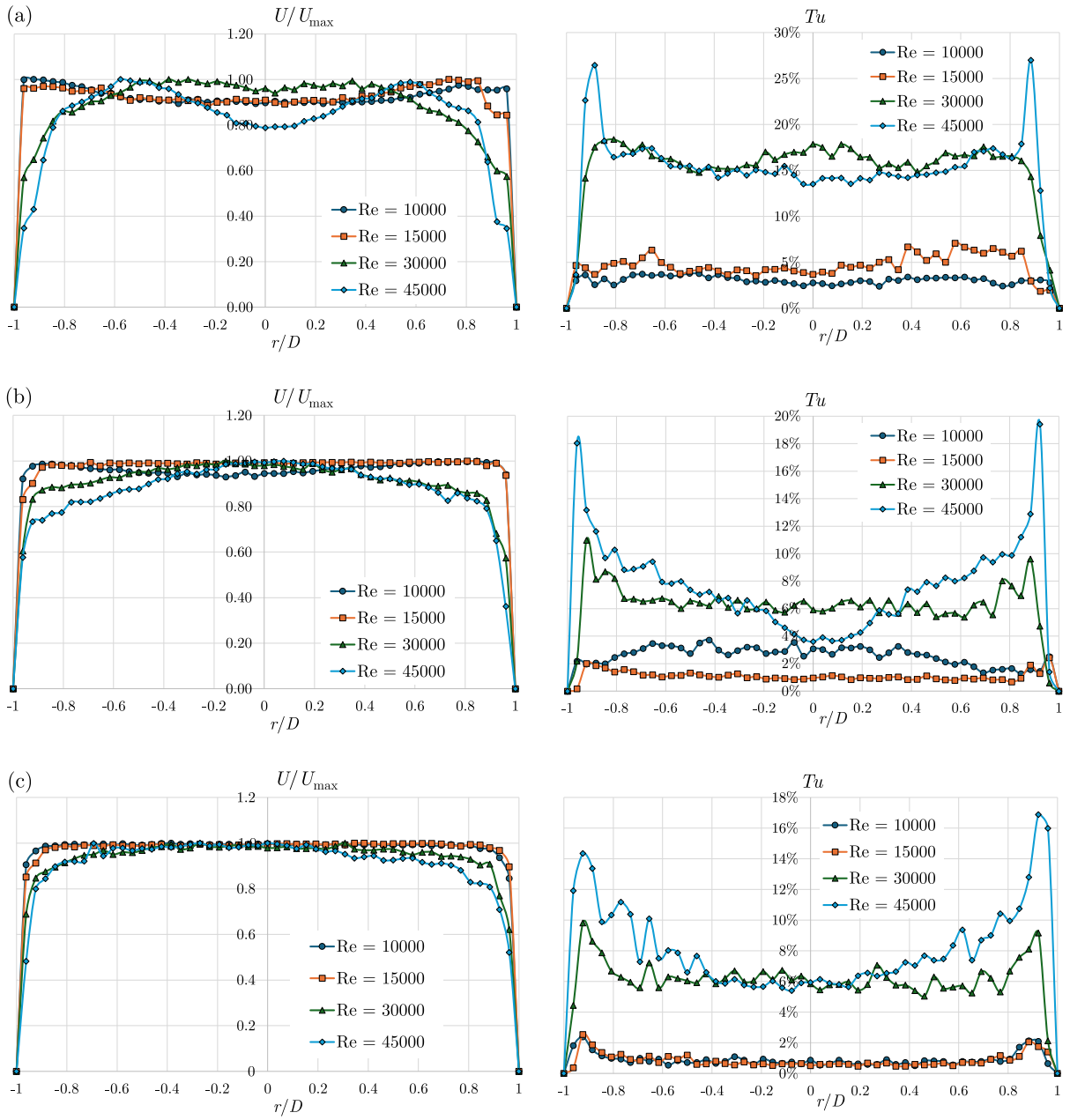

Fig. 2. Velocity (left) and turbulence intensity (right) in the outlet of the fun (a), 1000 mm behind the fun (b), and 2000 mm behind the fun (c).

3.2. Profiles at different straightener lengths

Figure 3 presents the velocity and turbulence profile measured 1000 mm downstream of a straightener for different straightener lengths and Reynolds numbers. At low Reynolds numbers (Figs. 3a and 3b), the impact of the straightener is minimal, with velocity profiles remaining nearly identical regardless of the straightener's length or presence. In terms of turbulence intensity, minor yet noticeable changes were observed. A significant reduction in turbulence intensity was detected near the duct wall at Re = 10000. At this Reynolds number, turbulence intensity decreased for all tested straightener lengths. However, the change was not substantial, as turbulence intensity remained below 1 % even without a straightener. At Re = 15000, no turbulence intensity was observed near the wall. However, for straighteners of 10 mm or longer, a decrease of approximately 0.25 percentage points in turbulence intensity was noted near the axis ($-0.4 < r/D < 0.4$).

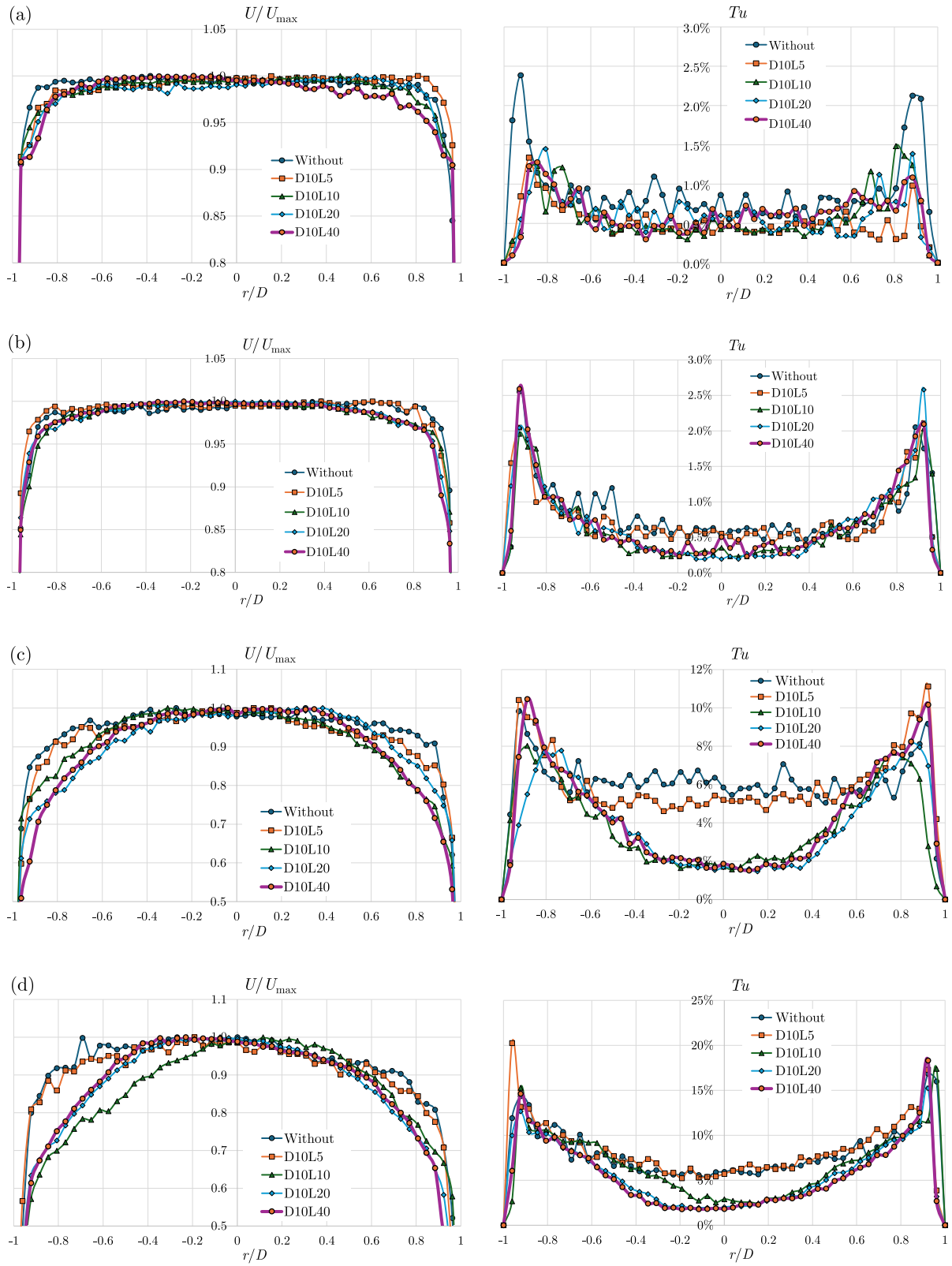

Fig. 3. Velocity (left) and turbulence intensity (right) profile at different Reynolds numbers and straightener lengths: (a) Re = 10000; (b) Re = 15000; (c) Re = 30000; (d) Re = 45000.

The use of the honeycomb straighteners had a significant influence on the shape of the velocity profile at Re = 30000. The longer the straightener, the more rounded and less squared the measured velocity profile becomes. This is evident from the reduced velocity values near

the duct walls ($r/D > \pm 0.4$). Turbulence intensity near the axis decreased for all investigated straighteners – by about 1 percentage point for L10D5, and approximately 4 percentage points for the remaining configurations. However, an increase in turbulence intensity near the duct walls was observed for D10L5 and D10L40.

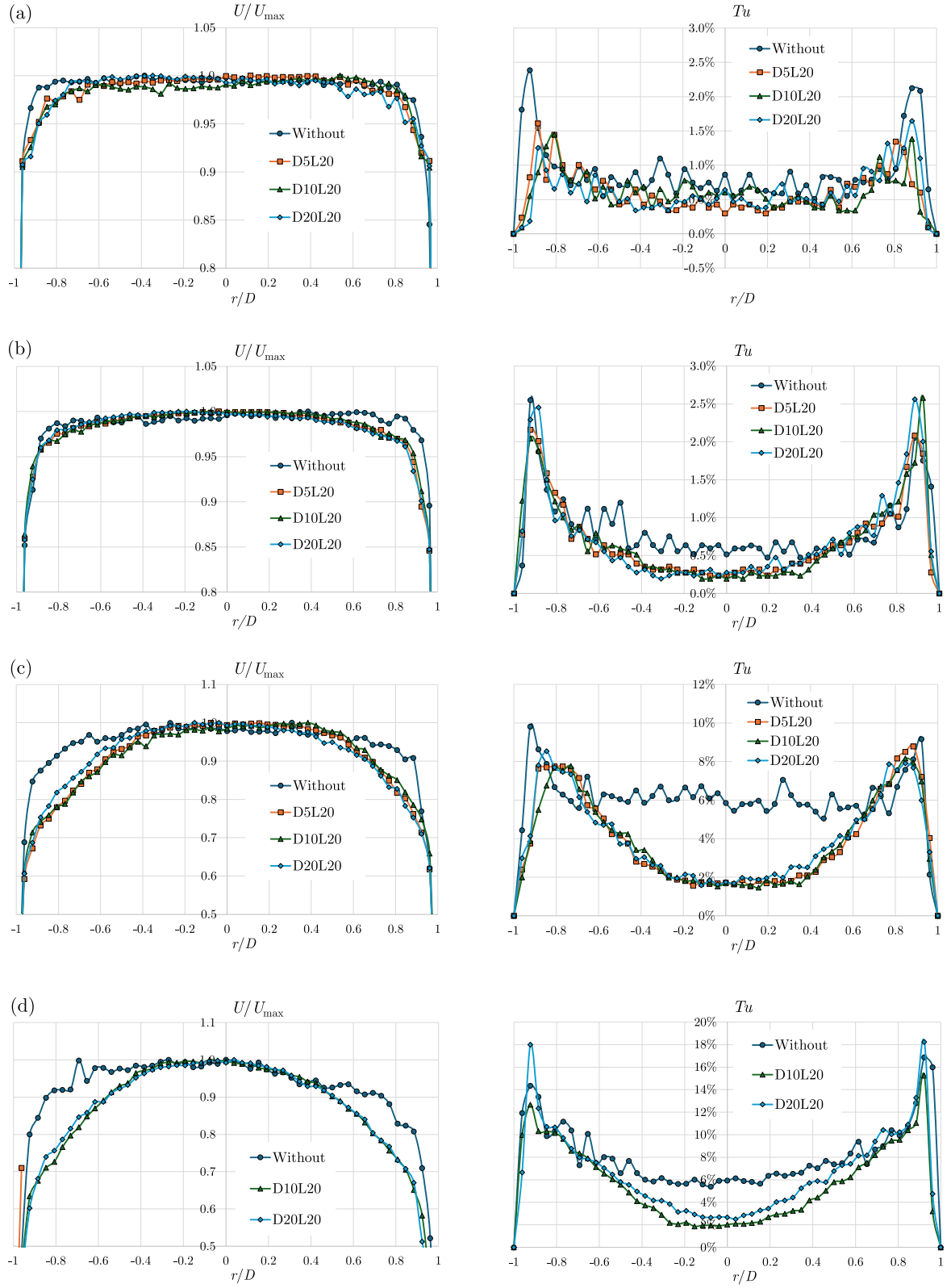

Fig. 4. Velocity (left) and turbulence intensity (right) profile at different Reynolds numbers and honeycomb diameters: (a) Re = 10000; (b) Re = 15000; (c) Re = 30000; (d) Re = 45000.

At Re = 45000, the impact of honeycomb straighteners on the velocity profiles was similar to that at Re = 30000. Again, longer straighteners resulted in more rounded velocity profiles, while the L10D5 configuration produced a noticeably asymmetric profile. Turbulence intensity decreased for all cases except the shortest straightener D10L5. Along the axis, the reduction in turbulence intensity decreased by about 3.03 percent point in the case of L10D10, 3.91 percent point in the case of L10D20, and 4.10 percent point in the case of L10D40. The profile asymmetry observed in the D10L10 case was reflected in its turbulence intensity.

3.3. Profiles at different honeycomb diameters

The velocity and turbulence intensity profiles at different Reynolds numbers and honeycomb sizes are presented in Fig. 4. At Re = 10000, the straighteners had no significant impact on either the velocity or turbulence intensity profiles. A slight decrease in both velocity and turbulence intensity was observed near the duct wall. The smaller the honeycomb, the lower the turbulence intensity, although the difference was minimal. At Re = 15000, the velocity profile was more symmetrical in ducts equipped with honeycomb straighteners. The turbulence intensity near the duct axis decreased by approximately 0.25 percentage points, regardless of honeycomb size.

At Re = 30000, the use of the honeycomb straightener influenced the velocity profile and turbulence intensity similarly across all honeycomb diameters. The velocity profile became more rounded, and turbulence intensity decreased by approximately 4 percentage points. Comparable results were obtained at Re = 45000. The measurement for the D5L20 was not included in Fig. 4d, as the experimental setup shown in Fig. 1 could not maintain a uniform flow for the duration required to capture the velocity profile data for this configuration.

3.4. Pressure drop on the straightener

Figure 5 shows the pressure drop measured over 1 meter of the duct where the straighteners were installed. The lowest pressure drop was recorded for the empty channel while the installation of any straightener resulted in increased hydraulic resistance. However, at Re = 10000, the drops were similar across all tested configurations. The lowest pressure drop was obtained for the D20L20 straightener. In general, a smaller honeycomb diameter corresponds to a higher pressure drop. The pressure drops for D10L20, D10L10, and D10L40 were identical, indicating that increasing the straightener length did not significantly affect the pressure loss. However, for the shortest straightener D10L5, higher losses were noted. These results indicate that, in addition to the typical pressure drop associated with the presence of shear stresses at the wall-air interface, straighteners can generate other disturbances that cause pressure drops. The research methodology used in this paper cannot indicate the nature of these phenomena. The highest pressure loss was shown for the D5L20 straightener, i.e., the straightener with the smallest diameter of the honeycomb.

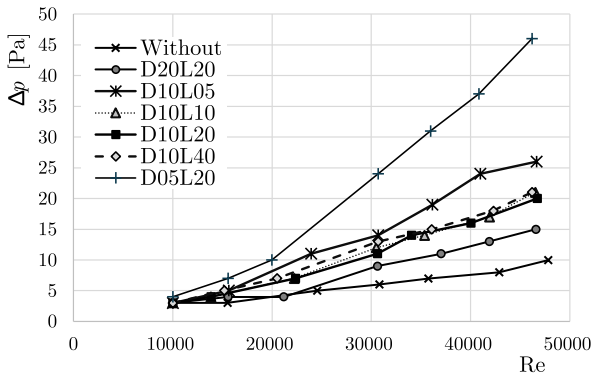

Fig. 5. Pressure drop in a honeycomb straightener for different Reynolds numbers.

4. Discussion

Figure 6 presents the relationship between axis turbulence intensity and the type of straighteners used. In all cases, the use of the honeycomb straightener resulted in a reduction in axial turbulence intensity. However, at low Reynolds numbers (Re = 10000 and Re = 15000), the reduction was minimal – 0.6 percentage points – regardless of the straightener configuration. Therefore, the use of flow straighteners at low Reynolds numbers appears unjustified. Despite their ineffectiveness, they introduce significant pressure losses in the system – exceeding 200 % at Re = 15000 for the D05D20 configuration (Fig. 5).

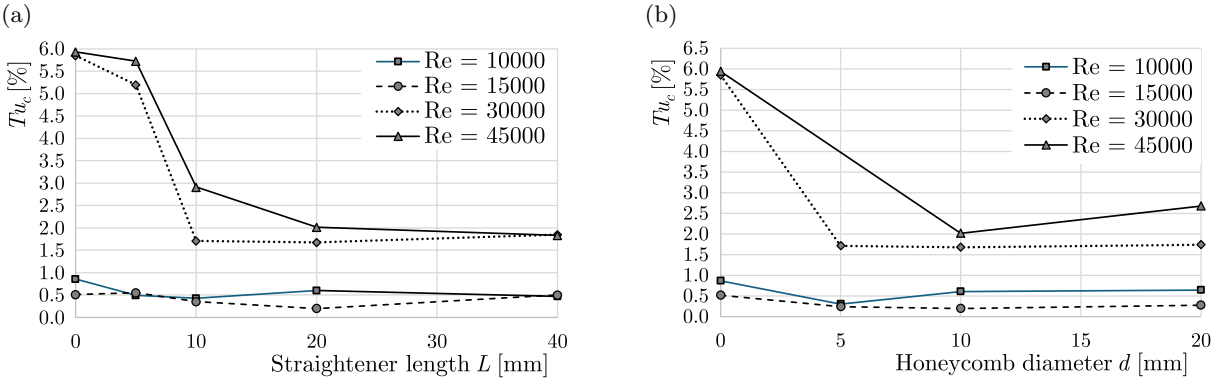

Fig. 6. Axis turbulence intensity for straighteners with different lengths (a) and honeycomb diameter (b).

At Re = 30000 and Re = 45000, the straighteners reduced turbulence intensity by more than 60 %. The reduction in turbulence increased with the straightener length up to 20 mm, after which it stabilized. The lack of impact of the stream straightener was observed from length 10 mm at Re = 30000. It should therefore be assumed that the higher the Reynolds numbers, the longer straighteners are required to achieve effective flow conditioning. The increase in honeycomb diameter did not affect the turbulence intensity at Re = 30000. However, when increasing the diameter to 20 mm, the axial turbulence also increased at Re = 45000. These findings indicate that smaller honeycomb diameters are more effective in reducing turbulence. It is important to note, however, that smaller honeycomb diameters also result in higher pressure losses (Fig. 5). Therefore, a honeycomb diameter of 10 mm appears to offer the best balance between performance and pressure drop.

4.1. Velocity profile analysis

A suitable method for quantifying the impact of straighteners on the velocity profile has not been established. Kühnen *et al.* (2018) investigated flow relaminarization at Re $\leq$ 6000, while Marensi *et al.* (2019) examined the impact of velocity profile flattening on drag reduction. The use of flow straighteners resulted in increased pressure losses (Fig. 5). However, the accurate measurement of pressure drop in the duct is challenging – especially at short distances – due to the need for highly precise instrumentation. Therefore, we propose an alternative approach based on evaluating the exponent n, calculated under the condition defined in Eq. (2.4). The values of exponent n derived from the measured velocity profiles are presented in Table 2. It is commonly assumed that $n = 7$ corresponds to fully developed turbulent flow (Salama, 2021). However, as shown in Table 2, the actual n values that best fit the experimental data are considerably higher. The values of n and the changes between them during the use of the straighteners only slightly reflect the observable changes in the shape of the velocity profiles. Therefore, Fig. 7 presents the percentage changes of the exponent n for the flow straighteners. Since the velocity profile is a function of the parameter $1/n$, the percentage change of parameter n presented in Fig. 7 was calculated as follows:

$$PCn = \frac{\frac{1}{n_i} - \frac{1}{n_{\text{without}}}}{\frac{1}{n_{\text{without}}}}, \tag{4.1}$$

where n_{without} is an exponent calculated for the velocity profile measured in the duct without straighteners, and n_i is an exponent calculated for the velocity profile measured in the duct with straighteners.

Table 2. Exponent n calculated for velocity profiles.

Reynolds number	Case						
	Without	D10L5	D10L10	D10L20	D10L40	D5L20	D20L20
10000	55.09	65.97	47.76	46.41	39.48	47.38	44.29
15000	50.97	54.94	37.22	37.17	34.52	34.92	21.25
30000	13.93	10.86	8.44	8.37	6.78	7.80	6.52
45000	9.50	8.47	5.28	5.28	5.26	–	5.28

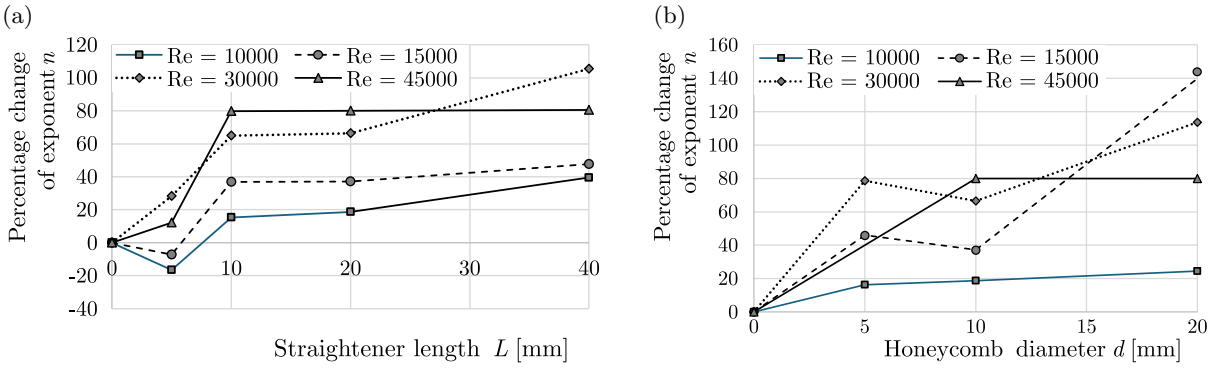

Fig. 7. Exponent n for different velocity profiles obtained for straighteners with different lengths (a) and honeycomb diameter (b).

The strongest impact of straighteners on the flow was observed at Re = 30000 and 45000. The percentage change in the exponent n was similar for all straighteners longer than 5 mm (Fig. 7a). In contrast, at Re = 10000 and 15000, the percentage change of the exponent n was negative – indicating that the value of the exponent n increased and the velocity profile became less laminar and more turbulent. These findings are consistent with the results reported by Xiong *et al.* (2003), who demonstrated that short straighteners (e.g., screens) initially cause an increase in turbulence level. For straighteners with different honeycomb diameters (Fig. 7b), an improvement in the velocity profile shape was observed in all cases. The highest percentage change in the exponent n occurred at Re = 15000, with a honeycomb diameter of $d = 20$ mm. Although this change is barely visible in the velocity profile (Fig. 4b), it is noteworthy that the use of the straightener reduced the n value from approximately 50.97 to 21.25. This is a large percentage change, but for high n values, it has little impact on the shape of the velocity profile.

The proposed method, based on the analysis of the exponent n, is relatively difficult to interpret. Therefore, an alternative approach is proposed, based on the kinetic energy correction factor, which can be calculated using the following formula:

$$\alpha = \frac{E_{\text{real}}}{E_{\text{ideal}}} = \frac{1}{A}\int_A \left(\frac{U(r)}{U_{\text{MEAN}}}\right)^3 \mathrm{d}A, \tag{4.2}$$

where E is the kinetic energy of the flow [J], A is a cross-section area of the duct $A = \frac{\pi D^2}{4}$ m^2, U_{MEAN} is a mean velocity in the duct [m/s].

Teleszewski (2018) showed that the kinetic energy correction factor is equal to 2 for the laminar flow, and approaches a value of 1 for fully turbulent flow. For this reason, it serves as a useful parameter for assessing changes in the shape of the velocity profile, which is directly related to the distribution of kinetic energy in the flow. Additionally, Teleszewski (2018) showed that the kinetic energy correction factor changes significantly within the Reynolds number range from 0 to 5000 ($\alpha(\mathrm{Re}=0)=2$ and $\alpha(\mathrm{Re}=5000)\approx 1.2$), but beyond this range the change is minimal $\alpha(\mathrm{Re}=20000)\approx 1.1$. Therefore, this parameter may be well-suited to evaluating the effect of a straightener on the flow profile. The calculated kinetic energy correction factors are presented in Fig. 8. For Reynolds numbers of 10000 and 15000, the use of a flow straightener had no noticeable effect on this parameter. This observation aligns with the velocity profile analysis, which also indicated minimal influence of the straighteners on the velocity profiles at these Reynolds numbers (Figs. 3a, 3b and Figs. 4a, 4b). The longer the straightener and the smaller the honeycomb diameter, the higher kinetic energy correction factor is observed at Re = 30000 and 45000. The largest increase in the parameter change is observed for the length of 10 mm and the diameter of 5 mm. At Re = 30000 and $d = 10$ mm, a decrease in the kinetic energy correction factor was observed.

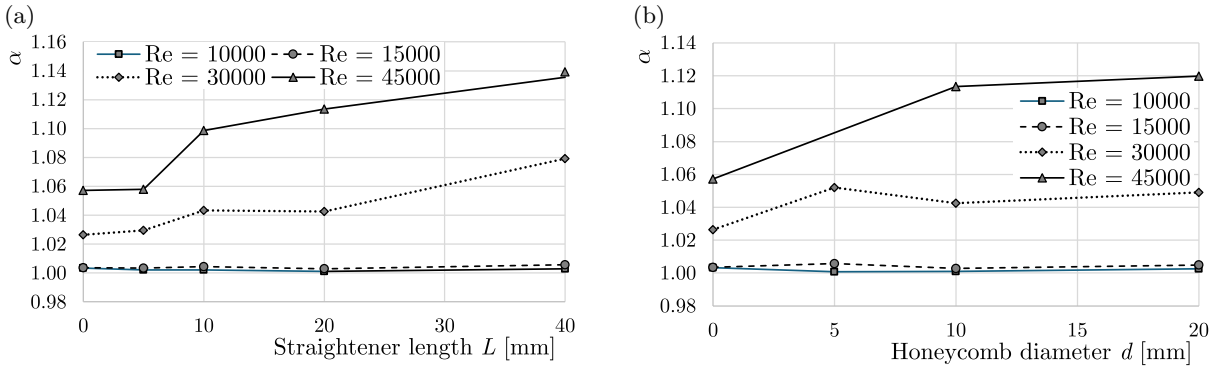

Fig. 8. Kinetic energy correction factor for different velocity profiles obtained for straighteners with different lengths (a) and honeycomb diameters (b).

An increase in the Reynolds number led to a decrease in the exponent n and an increase in the kinetic energy correction factor for cases without straighteners. While in a fully developed flow, the opposite trends would typically be observed and expected. However, in the present study, the flow is not fully developed, and shear stresses play a dominant role in altering the flow characteristics. As the Reynolds number increases, so does shear stress, resulting in a more rapid development of the velocity profile. This, in turn, influences the measured values of both the exponent n and the kinetic energy correction factor.

4.2. Minor loss coefficient of straighteners

Based on the measured pressure drop (Fig. 5), the major loss coefficient of the duct (Fig. 9a) and the minor loss coefficient of the straighteners (Fig. 9b) were calculated. The methodology for calculating loss coefficients is described in papers and several sources (Asker *et al.*, 2014). The minor loss coefficient of the straighteners was found to depend on the Reynolds number; however, no clear trend was observed. The highest minor loss coefficient was observed for the D05L20 straightener, while the lowest was for D20L20. The coefficients for D10L10, D10L20, and D10L40 straighteners were similar and, unexpectedly, lower than the shortest straightener D10L05. This suggests that the length of the straightener has a relatively minor influence on flow resistance. The D10L05 configuration may induce flow disturbances downstream, particularly at high Reynolds numbers, leading to additional losses. However, this hypothesis should be further validated using flow visualization techniques or particle image velocimetry (PIV). Among all

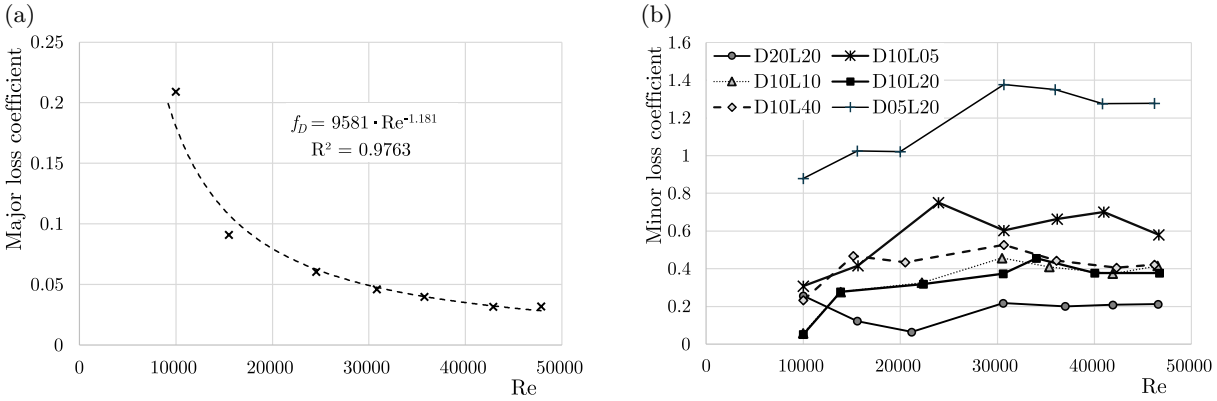

Fig. 9. Major loss factor in a straight duct (a) and the minor loss coefficient of straighteners (b).

parameters, the honeycomb diameter appears to exert the greatest influence on the minor loss coefficient.

It should be noted that the straightener reduces the cross-sectional flow area by introducing additional resistance surfaces – specifically, the front walls of the honeycomb cells. In the cases of D10L05, D10L10, D10L20, and D10L40, the reduction in flow area is identical, which explains the similar minor loss coefficients observed. The total wall surface area is the lowest for the D20L20 configuration and the highest for D05L20. This is due to maintaining the same wall thickness of 1 mm for all straighteners, rather than maintaining a constant flow area. Therefore, future research should include tests on straighteners with identical geometric dimensions (diameter and length) but varying wall thicknesses to better understand the influence of wall geometry on flow resistance.

5. Conclusions

The hot-wire anemometer was used to measure velocity profiles in a straight duct, both with and without a honeycomb straightener. Measurements were taken 1 meter downstream of the straightener and 2 meters downstream of the axial fan, which served as a turbulence generator. Additional measurements were also conducted at the fan outlet and 1 meter downstream of the fan. This study investigated the influence of the straightener length and honeycomb cell diameter on turbulence intensity, velocity profile, and pressure drop. Two methods were proposed to analyze the effect of the straightener on the velocity profile: the first is based on changes in the exponent n, while the second one utilizes the kinetic energy correction factor.

Based on the presented results and discussion, the following general conclusions can be drawn:

- the use of straighteners is primarily justified at high Reynolds numbers (Re = 30000, 45000), where the turbulence intensity is high and its decrease is most significant;
- straighteners influence the flow velocity profile at high Reynolds numbers, making it more parabolic and less rectangular – an effect referred to as flow relaminarization. The change in the profile shape can be quantified by analyzing the exponent n or the kinetic energy correction factor;
- even very short stream straighteners can reduce the level of flow turbulence, although as the straightener length increases, the reduction in turbulence intensity may increase (up to a certain point);
- as the honeycomb diameter increases, the straightener efficiency decreases;
- the honeycomb diameter has a greater influence on flow resistance than the straightener length. Notably, short straighteners ($l = 5$ mm) can induce higher pressure losses compared to longer ones.

The results presented in this study can serve as practical guidelines for the design of stream straighteners. The comprehensive dataset - including velocity and turbulence intensity profiles – can support further simulations aimed at extending this research. The analytical methods used to assess the velocity profile shape, such as the exponent n and kinetic energy correction factor, can also be compared with other approaches, including those based on major loss coefficient analysis. Finally, this study highlights promising directions for further research.

References

1. Asker, M., Turgut, O.E., & Coban, M.T. (2014). A review of non iterative friction factor correlations for the calculation of pressure drop in pipes. *Bitlis Eren University Journal of Science and Technology*, *4*(1), 1–8. https://dergipark.org.tr/tr/download/article-file/40279
2. Bradshaw, P. (1965). The effect of wind-tunnel screens on nominally two-dimensional boundary layers. *Journal of Fluid Mechanics*, *22*(4), 679–687. https://doi.org/10.1017/S0022112065001064
3. Dróżdż, A., Sokolenko, V., & Elsner, W. (2025). Performance analysis of novel wavy-wall-based flow control method for wind turbine blade. *Experimental Thermal and Fluid Science*, *169*, Article 111527. https://doi.org/10.1016/j.expthermflusci.2025.111527
4. Dutta, P., Rajendran, N.K., Cep, R., Kumar, R., Kumar, H., & Nirsanametla, Y. (2025). Numerical investigation of Dean vortex evolution in turbulent flow through 90° pipe bends. *Frontiers in Mechanical Engineering*, *11*. https://doi.org/10.3389/fmech.2025.1405148
5. El Drainy, Y.A., Saqr, K.M., Aly, H.S., & Jaafar, M.N.M. (2009). CFD analysis of incompressible turbulent swirling flow through Zanker plate. *Engineering Applications of Computational Fluid Mechanics*, *3*(4), 562–572. https://doi.org/10.1080/19942060.2009.11015291
6. Groth, J., & Johansson, A.V. (1988). Turbulence reduction by screens. *Journal of Fluid Mechanics*, *197*, 139–155. https://doi.org/10.1017/S0022112088003209
7. Hamzah, H., Jasim, L.M., Alkhabbaz, A., & Sahin, B. (2021). Role of honeycomb in improving subsonic wind tunnel flow quality: Numerical study based on orthogonal grid. *Journal of Mechanical Engineering Research and Developments*, *44*(7), 352–369.
8. Hrúz, M., Pecho, P., & Bugaj, M. (2020). Design procedure and honeycomb screen implementation to the Air Transport Department's subsonic wind tunnel. *AEROjournal*, *16*(2), 3–8. https://doi.org/10.26552/aer.C.2020.2.1
9. Hwang, Y. (2024). Near-wall streamwise turbulence intensity as $\mathrm{Re}_\tau \to \infty$. *Physical Review Fluids*, *9*(4), Article 044601. https://doi.org/10.1103/PhysRevFluids.9.044601
10. International Organization for Standardization. (2022). *Measurement of fluid flow by means of pressure differential devices inserted in circular cross-section conduits running full – Part 1: General principles and requirements* (ISO Standard No. 5167-1:2022). https://www.iso.org/standard/79179.html
11. Jurga, A.P., Janocha, M.J., Ong, M.C., & Yin, G. (2024). Numerical investigations of turbulent flow through a 90-degree pipe bend and honeycomb straightener. *Journal of Fluids Engineering*, *146*(2), Article 021307. https://doi.org/10.1115/1.4064101
12. Kaminski, K., Znaczko, P., Kardas-Cinal, E., Chamier-Gliszczynski, N., Koscielny, K., & Cur, K. (2025). Comparison of the heat transfer efficiency of selected counterflow air-to-air heat exchangers under unbalanced flow conditions. *Energies*, *18*(1), Article 117. https://doi.org/10.3390/en18010117
13. Klotz, L., Bukowski, K., & Gumowski, K. (2024). Influence of porous material on the flow behind a backward-facing step: experimental study. *Journal of Fluid Mechanics*, *998*, Article A31. https://doi.org/10.1017/jfm.2024.639
14. Kühnen, J., Scarselli, D., Schaner, M., & Hof, B. (2018). Relaminarization by steady modification of the streamwise velocity profile in a pipe. *Flow, Turbulence and Combustion*, *100*(4), 919–943. https://doi.org/10.1007/s10494-018-9896-4
15. Laws, E.M. (1990). Flow conditioning—A new development. *Flow Measurement and Instrumentation*, *1*(3), 165–170. https://doi.org/10.1016/0955-5986(90)90006-S

16. Lumley, J.L., & McMahon, J.F. (1967). Reducing water tunnel turbulence by means of a honeycomb. *Journal of Basic Engineering*, *89*(4), 764–770. https://doi.org/10.1115/1.3609700

17. Marensi, E., Willis, A.P., & Kerswell, R.R. (2019). Stabilisation and drag reduction of pipe flows by flattening the base profile. *Journal of Fluid Mechanics*, *863*, 850–875. https://doi.org/10.1017/jfm.2018.1012

18. Salama, A. (2021). Velocity profile representation for fully developed turbulent flows in pipes: A modified power law. *Fluids*, *6*(10), Article 369. https://doi.org/10.3390/fluids6100369

19. Saunders, G.P., Muller, S., Geierman, R., Duell, E., & Wagner, D.A. (2004). Wake effects of honeycomb stiffeners. *24th AIAA Aerodynamic Measurement Technology and Ground Testing Conference*. AIAA. https://doi.org/10.2514/6.2004-2199

20. Smyk, E., Stopel, M., & Szyca, M. (2024). Simulation of flow and pressure loss in the example of the elbow. *Water*, *16*(13), Article 1875. https://doi.org/10.3390/w16131875

21. Sun, K., Sun, J., Fan, Y., Yu, L., Chen, W., Kong, X., & Yu, C. (2023). Characterization of a synthetic jet vortex ring flowing through honeycomb. *Physics of Fluids*, *35*(7), Article 075123. https://doi.org/10.1063/5.0155935

22. Sun, K., Zhang, S., Shi, N., Peng, S., Cao, J., Sun, J., & Chen, W. (2025). Experimental investigation of synthetic jet impingement upon a honeycomb. *European Journal of Mechanics – B/Fluids*, *111*, 319–333. https://doi.org/10.1016/j.euromechflu.2025.02.003

23. Tan-Atichat, J., Nagib, H.M., & Loehrke, R.I. (1982). Interaction of free-stream turbulence with screens and grids: a balance between turbulence scales. *Journal of Fluid Mechanics*, *114*, 501–528. https://doi.org/10.1017/S0022112082000275

24. Teleszewski, J.T. (2018). Experimental investigation of the kinetic energy correction factor in pipe flow. *E3S Web of Conferences*, *44*, Article 00177. https://doi.org/10.1051/e3sconf/20184400177

25. Xiong, W., Kalkühler, K., & Merzkirch, W. (2003). Velocity and turbulence measurements downstream of flow conditioners. *Flow Measurement and Instrumentation*, *14*(6), 249–260. https://doi.org/10.1016/S0955-5986(03)00031-1

Manuscript received May 28, 2025; accepted for publication July 21, 2025; published online October 7, 2025.